VOLUME MESH ADAPTATION WITH A MESHFREE SURFACE MODEL

A. Rassineux, P. Breitkopf, C. Chappuis, P. Villon

Université de Technologie de Compiègne, Laboratoire Roberval, Centre de Recherches de Royallieu, BP20529, 60206 Compiègne Cedex, France

ABSTRACT

We present a method to adapt a tetrahedron mesh together with a surface mesh with respect to a size criterion. Both surface and tetrahedron mesh adaptation are carried out simultaneously and no CAD is required to adapt the surface mesh. The adaptation procedure consists in splitting or removing interior and surface edges in order to enforce a given size criterion. The enrichment process is based on a bisection technique. Mesh conformity during the refinement process is guaranteed since all possible remeshing configurations of tetrahedra are examined. Surface nodes are projected on a geometrical model once the tetrahedron mesh has been adapted. The building of a surface model method is based on a meshfree technique denoted as Hermite Diffuse Interpolation. Surface and volume mesh optimization procedures are carried out during the adaptation and at the end of the process to enhance the mesh.

Keywords: Tetrahedral meshes; mesh refinement; mesh adaptation

1. INTRODUCTION

The process involved in mesh adaptation techniques[1] is iterative. Once an initial coarse mesh is created, a first solution is obtained and an error sensitivity analysis can be performed in order to calculate the density of the optimal mesh. When the densities of the optimal mesh have been computed, a new surface mesh which respects the prescribed density is created and the volume is meshed with respect to both size and shape of the elements. Several authors have proposed techniques to adapt surface or tetrahedron meshes [2-4]. These two steps, namely surface and volume adaptation, are usually carried out independently[3,5]. In this paper, we present a method which combines simultaneous surface and tetrahedron adaptation at a reasonable computational cost. We first introduce our enrichment procedure based on bisection. The building of the surface geometry based on Hermite diffuse interpolation[5-7], HDI is briefly reminded. Finally, we present how local surface and volume mesh optimization procedures have been coupled. Representative examples are discussed at the end of the paper.

2. MESH QUALITY CRITERIA

We define some measures of both shape and size quality of a tetrahedron or a triangle.
The shape quality criterion for a tetrahedron (or a triangle) is defined as follows

$$Qe(T) = \alpha \times \frac{\rho}{h} \qquad (1)$$

where h is the longest edge length of the element
ρ is the ratio of the radius of the sphere (or the circle) inscribed in the element
A coefficient α is applied so that the criterion of an equilateral element is set at 1.
The size quality criterion of an edge is defined as follows

$$Qt(A) = min(\frac{h_{th}}{h}, \frac{h}{h_{th}}) \quad and \quad 0 \le Qt(A) \le 1 \qquad (2)$$

h is the length of the edge.
h_{th} is the density of the mesh provided by the error estimation procedures.

3. TETRAHEDRON MESH ADAPTATION

Rivara [8-10] has presented refinement techniques during which mesh quality is controlled and has given mathematical and numerical evidence of methods based on the longest-side refinement. These methods greatly improve the refinement and derefinement of unstructured triangulations. The author has also introduced methods suitable for constrained Delaunay triangulations and has presented an improvement of the longest-side refinement based on a Side Propagation Path concept. An extension to 3D meshes of the Longest-Edge Propagation Path of the worst triangles of a triangulation has also been proposed. A 8-tetrahedra longest-edge algorithm which generalizes the 4 triangles longest-edge refinement algorithm is explained and statistical and fractal non-degeneracy properties over this 3D refinement algorithm are proved. A study shows that the volume percentage covered by better tetrahedra is improved. We do not pretend to compare our mesh refinement technique with Rivara's techniques during which mesh quality is controlled as we have decided to separate mesh refinement algorithm and shape quality requirements. However, we perform a further treatment to improve the quality of the mesh. The refinement of the mesh is carried out by splitting edges at the middle. Edges which must be split are identified (size criterion <0.66). In a first step, we consider that the mesh to adapt is composed of a set of independent triangular faces. Once the new contour of each face is determined, each face can be remeshed. Most authors [4,11,12,13] have limited the number of patterns and therefore have proposed solutions to ensure mesh conformity. We have decided to identify all existing subdivision patterns of tetrahedra in order to solve problems related to mesh conformity. We present the main lines of the algorithm.

3.1 Mesh size

Element size distribution is provided by a grid constituted of an initial tetrahedron mesh. In order to validate our work, we give an explicit size function. However, the criterion size has been computed at each node of the initial mesh in order to simulate what occurs during a typical adaptation process. The adaptation procedure consists in splitting or removing interior and surface edges which violate the given size criterion.

3.2 Subdivision of faces

A tetrahedron is made of a set of 4 faces. Each face is composed of 3 edges. Each face can be remeshed as shown in figures 1. 11 patterns have been identified.

The set of triangles provided by the refinement of the four faces of a tetrahedron element can be seen as the envelope of a volume to mesh (between 4 and 16 faces). The main idea of the adaptation process consists of remeshing each sub-volume using a pre-computed pattern of tetrahedra. We have used our advancing front mesh generator[3] to determine automatically all different patterns which can be found. We have determined 239 different configurations. We have also classified manually and counted all different patterns but we shall not detail this point in this paper. A program which writes in a data file all remeshing configuration has been written. Once all patterns of tetrahedra have been computed, each skin mesh is given a unique code as well as a corresponding pre-computed set of tetrahedra. When two of the three edges of a face must be split, the face is divided into 3 triangles. Figures 1 show that the face can be remeshed in two different ways. A shape criterion of each triangle is calculated and decision is made with respect to this criterion.

3.3 Triangular mesh patterns

The different configurations of faces can be classified with respect to the interior edges that can be created inside the face. As shown in figures 1, 6 interior edges can be created what leads to 24 possible edges for a tetrahedron.

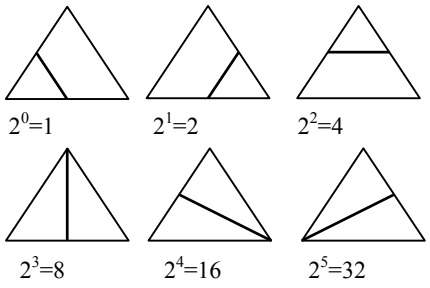

Figures 1 : 6 interior edges can be created. Edge i is given the code 2^i

Using this strategy, sub-meshes of faces can be numbered as shown in figures 2.

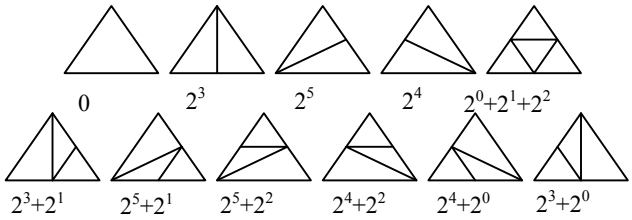

Figures 2 : Remeshing of a face and associated code.

3.4 Local remeshing of a tetrahedron

Each tetrahedron is given the following code

$$Code = \sum_{i=0}^{i=3} FaceCode(i) \times 2^{6 \times i} \qquad (3)$$

We propose on figures 3 an example of remeshing and the associated code. The code of the configuration shown figures 3 is given by

$$Code = 20 \times 2^0 + 8 \times 2^6 + 20 \times 2^{12} + 7 \times 2^{18} = 1917460$$

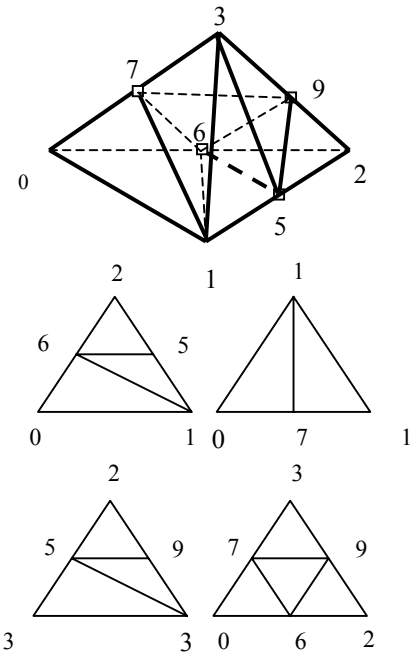

Figures 3 : Computation of the skin mesh code for a given configuration

Since all possibilities are identified, the adaptation process is instantaneous.

We do not detail all configurations of tetrahedra but we propose to focus on patterns in which a node must be added. The generation of tetrahedra inside a given set of faces is not always guaranteed and sometimes an additional node must be created[3]. These configurations are known as Schönhart polyhedra[14] and lead to a decomposition into 9, 10 or 11 tetrahedra as shown in figures 4.

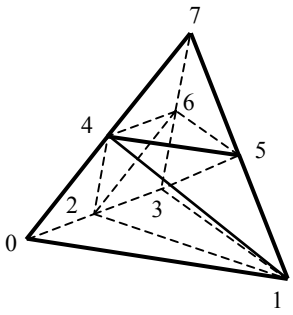

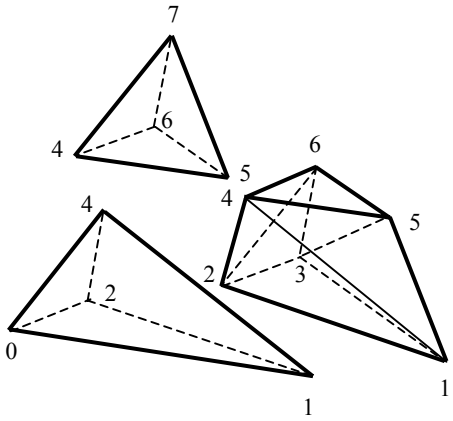

Figures 4 : Remeshing into 10 tetrahedra. The volume is decomposed into a Schönhart polyhedron remeshed into 8 tetrahedra and 2 tetrahedra

We observed that a lower memory and a much better computational costs can be obtained with our method as no special post-treatment is required to ensure the conformity of the mesh. As a counterpart, the computational time is spent in the shape optimization procedures performed at the end of each refinement step and at the end of the final adaptation process.

3.4. Pattern classification

In order to validate our work, we propose to classify and count all different patterns.
The relationship between the faces of the tetrahedron and the edges is given figure 5 and table 1.

We note ijk, the face composed of edges i, j and k. If edge i is split, the edge is noted $\underline{i}$.

Let us first consider the remeshing contours of face F_0.
The contours can be described as 123 (no edge split), $\underline{1}23$, $1\underline{2}3$, $12\underline{3}$ (one split edge), $\underline{12}3$, $1\underline{23}$, $\underline{1}2\underline{3}$ (2 split edges) and $\underline{123}$ (3 split edges). For each configuration of face F_0 (8 configurations), an array shown in table 2 is built. Once the columns of F_1 corresponding to edges 4 and 5 have been filled, the column of face F_2 corresponding to edge 5 is imposed. At last, edge 6 may be split or not. Then, the nodes on the contour of face F_3 are fully determined. R_0, R_1, R_2 and R_3 denote the number of possible remeshing configurations of the respective faces F_0, F_1, F_2, and F_3 with respect to the given contour.
The number of remeshing configuration R for a given contour discretization of the faces is given by the product $R_0R_1R_2R_3$.
When the contour of a face contains 2 new nodes, the contour can be meshed by two different manners. Otherwise (0,1 or 3 additional nodes), only one configuration is possible.

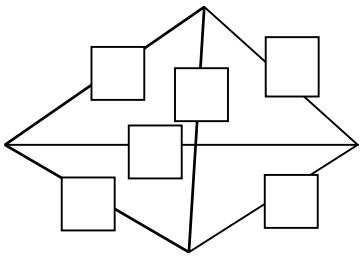

Figure 5: Link between faces and edges inside a tetrahedron

Face	Node numbers					
0	0	4	1	5	2	6
1	0	7	3	8	1	4
2	1	8	3	9	2	5
3	0	6	2	9	3	7

Table 1 : Definition of faces

Edges of Face 0	Edges of Face 1			Edges of Face 2			Edges of Face 3			R_0	R_1	R_2	R_3	R
	1	4	5	2	5	6	3	4	6	1	1	1	1	1
	1	4	5	2	5	6	3	4	6	1	1	1	1	1
	1	4	5	2	5	6	3	4	6	1	1	1	1	1
123	1	4	5	2	5	6	3	4	6	1	1	2	1	2
	1	4	5	2	5	6	3	4	6	1	1	1	1	1
	1	4	5	2	5	6	3	4	6	1	1	1	2	2
	1	4	5	2	5	6	3	4	6	1	2	1	1	2
	1	4	5	2	5	6	3	4	6	1	2	2	2	8
Number of configurations 18														
	1	4	5	2	5	6	3	4	6	1	1	1	1	1
	1	4	5	2	5	6	3	4	6	1	1	1	1	1
123	1	4	5	2	5	6	3	4	6	1	2	1	1	2
	1	4	5	2	5	6	3	4	6	1	2	2	1	4
	1	4	5	2	5	6	3	4	6	1	2	1	1	2
	1	4	5	2	5	6	3	4	6	1	2	1	2	4
	1	4	5	2	5	6	3	4	6	1	1	1	1	1
	1	4	5	2	5	6	3	4	6	1	1	2	2	4
Number of configurations for 123, 123, 123 = 19 × 3= 57														
	1	4	5	2	5	6	3	4	6	2	1	1	1	2
	1	4	5	2	5	6	3	4	6	2	1	2	1	4
123	1	4	5	2	5	6	3	4	6	2	2	2	1	8
123	1	4	5	2	5	6	3	4	6	2	2	1	1	4
123	1	4	5	2	5	6	3	4	6	2	2	1	1	4
	1	4	5	2	5	6	3	4	6	2	2	2	2	16
	1	4	5	2	5	6	3	4	6	2	1	2	1	4
	1	4	5	2	5	6	3	4	6	2	1	1	2	4
Number of configurations for 123, 123, 123 = 46 × 3= 138														
	1	4	5	2	5	6	3	4	6	1	1	1	1	1
	1	4	5	2	5	6	3	4	6	1	1	2	2	4
	1	4	5	2	5	6	3	4	6	1	2	2	1	4
123	1	4	5	2	5	6	3	4	6	1	2	1	2	4
	1	4	5	2	5	6	3	4	6	1	2	1	2	4
	1	4	5	2	5	6	3	4	6	1	2	2	1	4
	1	4	5	2	5	6	3	4	6	1	1	2	2	4
	1	4	5	2	5	6	3	4	6	1	1	1	1	1
Number of configurations = 26														
Total number of configurations = 239														

Table 2 : All skin mesh configurations. The column of face F_2 corresponding to edge 5 is fully determined by the discretization of F_1. Nodes on the contour of F3 are imposed by neighbor faces F_1 and F_2

3.6 Global remeshing

The process is iterative. Once edges of the initial mesh are examined, faces of the tetrahedra are split and tetrahedra are refined. A new tetrahedron mesh is created and the process is repeated until all edges have the desired size. At the issue of each refinement iteration, a shape optimization process is performed to remove ill shaped elements (shape criterion less than 0.2).

3.7 Shape enhancement procedures

Tetrahedron optimization procedures have been detailed by a large number of authors[2-4]. The method involves extracting sub-volumes from the tetrahedron mesh volume, which are then remeshed to improve their quality. The quality of a set of tetrahedra is that of the most distorted element. The sub-volumes are constructed by determining the outer faces of the set of tetrahedra which touch the same node, edge or face. Elements of which the quality criterion is below a value fixed a priori are selected and remeshed if possible to a higher criterion. A nodal shifting process[2] is applied at the end of the process.

4. SURFACE REMESHING BY HDI

The method has been fully detailed in reference[5] and we remind briefly the main lines of the technique. Volume mesh has been adapted and new nodes have been created. Surface nodes must be projected on the geometrical surface. The technique we propose is based on the polyhedral representation of the object by the mesh itself and therefore do not use the parameter space. A secondary geometrical model is built to achieve the adaptation. The geometrical support is build by a Moving Least Squares[15] approximation method on a local window denoted as HDI[5-7]. The objective is to determine a local surface equation using the nodes of the initial mesh and the normal vectors to the surface calculated from the mesh. The form of surface suited to the local diffuse interpolation is denoted as Monge patch of equation z=f(x,y) where f is a C2 function defined on a planar domain. The surface equation is evaluated through a second order equation. and can be expressed as

$$z = f(x,y) = < 1, x, y, x^2, xy, y^2 > \alpha = P^T \alpha \quad (4)$$

where α is a 6 coefficients vector.

Whenever a projection method on a mesh is used, the determination of a projection face may lead to ambiguous configurations. If the surface mesh contains ill shaped elements, the determination becomes even more difficult. Considering the discrete nature of the surface, we have extended our approach to clouds of points in order to eliminate numerical problems due to ambiguous configurations.

The diffuse approximation has been used to determine a projection plane whose coefficients vary continuously with respect to the point to project. We observed that both reliability and efficiency of the projection have been greatly improved. The outline of the method can be described as follows:

A set of n points $(x_1,x_2,\ldots,x_n)$ is given. These nodes are the n nearest nodes to the evaluation point X.

$$\mathbf{xd} = (xd, yd, zd) = \frac{1}{n}\sum_{i=1}^{i=n} w(\mathbf{x}i, \mathbf{x})\mathbf{x}i \tag{5}$$

We introduce a diffuse origin xd=(xd,yd,zd) of the set as **x**(x,y,z) is a node of the adapted mesh, we determine the plane which minimizes the following criterion

$$J\mathbf{x}(\mathbf{a}) = \frac{1}{2}\sum_{i=1}^{i=n} w(\mathbf{xi}, \mathbf{x})\{a(xi - xd) + b(yi - yd) + c(zi - zd)\}^2 \tag{6}$$

with aT = (a,b,c) under the constraint aT a=1

The problem can be written as

$$Min(\frac{1}{2}\mathbf{a}^{\mathrm{T}}\mathbf{P}^{\mathbf{T}}\mathbf{WPa}) \text{ with } \mathbf{a}^{\mathbf{T}}\mathbf{a} = 1 \tag{7}$$

where W is the diagonal matrix of the weights and

$$\mathbf{P} = \begin{bmatrix} x1 - xd & y1 - yd & z1 - zd \\ . & . & . \\ xn - xd & yn - yd & zn - zd \end{bmatrix}, n \times 3 \text{ matrix} \tag{8}$$

This problem is solved by determining the eigenvalues of PTWP matrix.

5. MESH OPTIMIZATION

Our method can been used to adapt an initial surface mesh as well as an existing tetrahedron mesh.
When only a surface mesh is provided, a traditional adaptation process is performed. The surface mesh is adapted with respect to both size and shape criteria and a tetrahedron mesh is performed and adapted thereafter. As the first step of our technique is based on bisection, much attention must be paid to the quality (shape and size) of both tetrahedron and surface meshes. Our procedure[3] also allows the mesh to be coarsened. The de-refinement of the mesh can be carried out in specified areas inside the volume and on the surface[5]. As far as the density of the surface mesh is coarser or somehow similar to the prescribed density, we observe that the existing mesh can be used at a lower computational cost than a full remeshing. Otherwise, if the distribution of elements on the surface is much finer than the optimal mesh, intensive use is made of the de-refinement procedure. In this particular case it may be more efficient to design a completely new mesh which satisfies the prescribed requirements at least in some areas of the model.

In a surface remeshing context[5], mesh optimization procedures are known as edge splitting, edge collapsing, edge swapping, vertex removing and nodal shifting. We have adapted to surface meshes on the HDI model a nodal shifting procedure introduced by George et al.[2]. As some points must be specified, the process is briefly reminded.

The procedure consists of shifting the point P step by step to an ideal position P_{opt} with respect to the n outer edges of the connected triangles. The solution point P_{opt} can be seen as the center of gravity of n ideal points $P_{id}(j)$ of each outer edge j. The weight at each point $P_{id}(j)$ is the inverse of the square of the quality criterion Q(Tj) of the triangle created with the edge j and its ideal point $P_{id}(j)$.

Thus, the iterative process can be written as

$$\begin{aligned} &P = P + d \text{ and } d = \alpha PP_{opt} \\ &\text{with } P_{opt} = \sum_{j=1}^{j=n} \beta_j P_{id}(j), \\ &\beta_j = \frac{\gamma}{Q(Tj)} \text{ and } \gamma = \frac{1}{\sum_{j=1}^{j=n} \beta_j} \end{aligned} \tag{9}$$

The process is performed in the diffuse approximation plane introduced in section 4. Points *Pid(j)* are calculated in the moving least squares plane but quality criteria are computed in the real space. At the issue of the iteration, the point is projected on the geometrical model.

The de-refinement procedures consist of remeshing the outer contour (or the surface mesh) constituted by all triangles (or tetrahedra) sharing the same node or the same edge.

Whenever a topological change occurs on the surface mesh, a corresponding set of tetrahedra is destroyed and the gap between the new surface mesh and the existing mesh is filled by our advancing front mesh generator. In a practical way, we have tried to minimize the number of topological changes on the surface mesh after the refinement process as we observed that the nodal shifting procedure proved to be really efficient. Once the enrichment iterations have been performed, nodes are projected on the diffuse model and the surface mesh is optimized. In a final step, the volume mesh is enhanced.

In the examples which follow in Figures 6, we illustrate the different steps of the enhancement procedures and the efficiency of the local remeshing operators applied on the HDI model.
The initial mesh is shown in figure 6a. A shape optimization procedure is first performed. The result is provided in figure 6b. The size of the mesh is optimized in a final step. Here, we imposed a constant size mesh shown in figure 6c. A tetrahedron mesh can be performed afterwards.

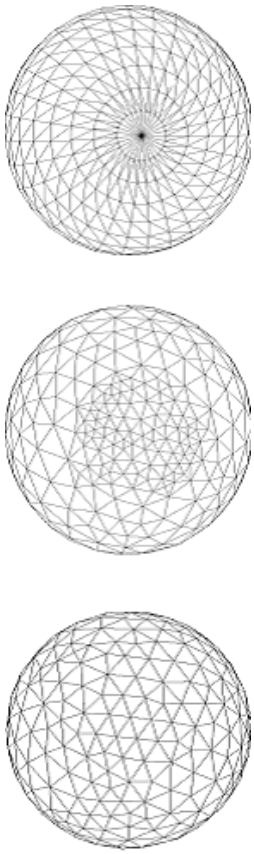

Figures 6: (a) : Initial mesh. (b) : Pre-optimized mesh. (c) Final mesh : a constant size mesh is requested.

6. RESULTS

The initial surface mesh used for all examples is shown in figure 8a. We have chosen a coarse mesh of a sphere in order to demonstrate the ability of HDI to respect the shape of the geometry. The initial tetrahedron mesh is made of 480 tetrahedra.

The radius of the sphere is R. The definition of the explicit size function is given in figures 7. Element size on the 3 cylinders of radius r is set at d_{min}. The cylinders have been displayed on figure 7a but they do not belong to the geometry. Element size of a point inside the sphere is given by the shortest distance to the cylinders. As shown on figure 7b, in each plane normal to the axis of the cylinders, the density is assumed to be linear and is given by

$$h(x) = \left(1 - \frac{x}{R}\right) \times d\,\min + \frac{x}{R} \times d\,\max \qquad (10)$$

where x denotes the radial distance to the cylinder in the projection plane. The element size is the smallest value of the density computed in each projection plane. dmax is set at R/3 in all examples.

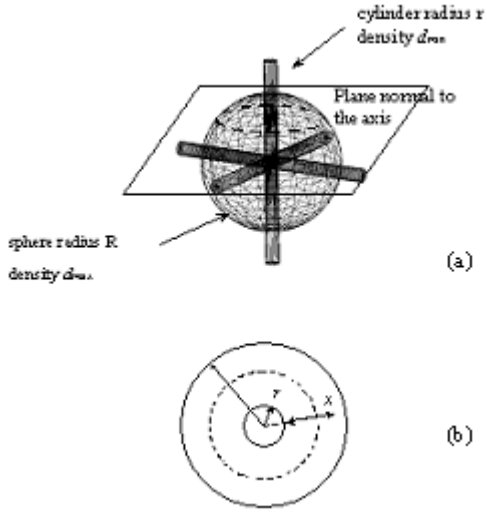

Figures 7 : Definition of the explicit element size distribution. Element size inside the sphere grows from dmin to dmax with respect to the shortest distance to the cylinders.

We observed that the computational time of our bisection technique alone is low (below 10% of the whole process) even for bigger models (4M tetrahedra). Results are provided in table 3. At the end of the final process, 100% of the elements have the desired size (size criterion >0.66). An optimization iteration is performed at the end of each tetrahedron mesh refinement iteration in order to remove elements the quality of which is below 0.2. We can consider that nearly the whole computational time is spent on the optimization process. We use a PC pentium III, 500Mhz. After the optimization, we observed that more than 80% of the elements have a shape quality criterion greater than 0.5. The shape quality criterion of all meshes is greater than 0.2. A further optimization at a higher shape criterion can be performed in a final step if needed.

d_{min}/	0.03	0.01	0.03	0.01	0.01
r/R	0.03	0.01	0.3	0.3	0.7
Nele	113197	417057	500068	1672 894	4103 420
Cpu	11 s	36 s	42 s	132 s	397 s
Qmin	0.20	0.20	0.20	0.20	0.20

Table 3 : Results. Element size distribution is controlled by the minimum required density on the cylinders dmin and by the radius r of the cylinders. Nele denotes the number of tetrahedra of the adapted mesh.

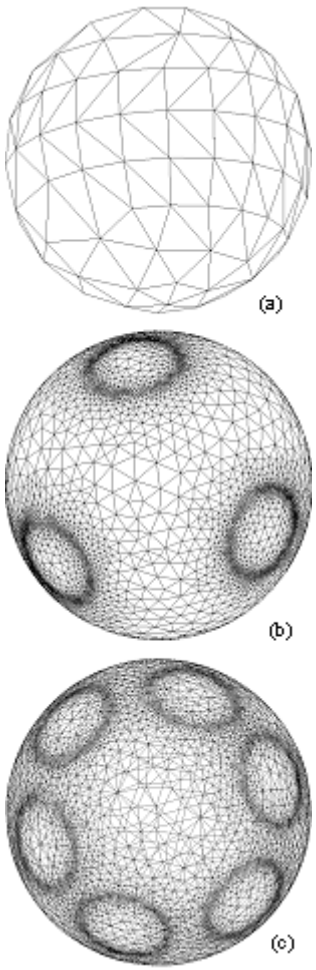

Figure 8: Initial model and illustration of the element size distribution. (a) : Initial tetrahedron mesh. (b) : Skin of the volume mesh. Parameters are dmin/R=0,01 and r/R=0,3. (c) : Wireframe surface mesh

On figures 8b, 8c, 9a, only the skin mesh has been represented. After the bisection process (fig 9a), nodes are projected on the HDI model. The result is shown in figure 9b. Surface and volume optimization procedures are combined together thereafter. Some elements of the volume mesh are displayed in figure 9c.

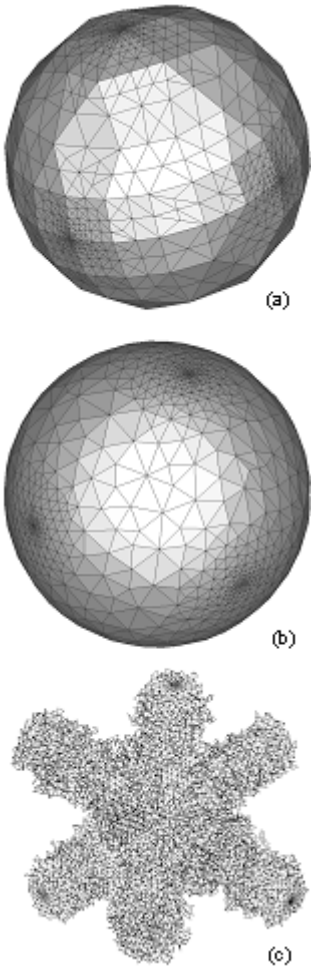

Figure 9: Projection on the HDI model and optimization procedures. Parameters are dmin/R=0,01 and r/R=0,01. (a) : Mesh obtained after the bisection process. (b) : Optimized mesh. Nodes are projected on the HDI model. (c) Volume elements the size of which is less than a given threshold t = 5dmin are displayed.

CONCLUSION

We proposed a method to adapt meshes with large number of elements with respect to size and shape requirements. Surface and volume refinement and derefinement techniques have been coupled successfully. The method shows that meshfree techniques are not restricted to problems which cannot be solved with finite elements and that both cultures can be used complementarily.

REFERENCES

[1] P. Beckers, H.G Zhong, Mesh adaptation for 2D stress analysis, 2nd International Conference on Computational Structures Technology, Athens Greece, Aug 30 - Sep 1, published in Advances in Post Processing for Finite Element Technology, 47-59, Civil Comp Ltd, Edinburgh, Scotland B.H.V, Edn. topping and Papadrakakis (1994).

[2] P.-L.George, F. Henot F., E. Briere de L' Isle, Optimisation de maillages tétraèdriques, Actes du Congrès StruCome 93, Paris, 1993.

[3] A. Rassineux,Generation and optimization of tetrahedral meshes by advancing front technique, Int. J. Num. Meth. in Eng., 41, 651-674 (1998).

[4] P-J. Frey, P-L. George, Maillages, applications aux éléments-finis, Hermes Science, (1999).

[5] A. Rassineux, P. Villon, J-M. Savignat, O.Stab,Surface remeshing by local Hermite diffuse interpolation, Int. J. Num. Meth., 49, 31-49, (2000).

[6] B. Nayroles B., G. Touzot, P. Villon, L'approximation diffuse, C.R.Acad. Sci, Paris, 313, II, 293-29 (1991).

[7] P. Breitkopf, A. Rassineux, G. Touzot, P. Villon, Explicit form and efficient computation of MLS shape functions and their derivatives, Int. J. Num. Meth., 48, 451-466, 2000

[8] M-C Rivara., Local Modification of Meshes for Adaptive and/or MultiGrid Finite-Element Methods, J. Computational. and App. Math., Elsevier, 36, 79-89, (1991).

[9] M-C Rivara, New Longest-Edge Algorithms For the Refinement and/or Improvement of Unstructured Triangulations, Int. J. Num. Meth., 40, 3313-3324, (1997).

[10] M.C. Rivara, A. Plaza, A.Longest-Edge Algorithms: Nondegeneracy Properties in 3 Dimensions, 5th US National Congress on Comp. Mech., 2nd Symposium on Unstructured Mesh Generation University of Colorado, Boulder, (1999).

[11] A. Plaza, G.F., Carey, About Local Refinement of Tetrahedral Grids based on Bisection, 5th Int. Meshing Roundtable, Sandia National Lab., 123-136, (1996).

[12] E. Bänsch, Local Mesh Refinement in 2 and 3 Dimensions, IMPACT of Computing in Science and Engineering, 3, 181-191, (1991).

[13] D. N. Arnold, A. Mukherjee,. Tetrahedral bisection and adaptive finite elements, Grid Generation and Adaptive Algorithms, IMA Volumes in Mathematics and its Applications, Springer-Verlag, New York-Heidelberg-Berlin, 113, 29-42, (1999).

[14] E. Schönhart, Über die Zerlegung von Dreieckspolyedern, Mathematish Annalen, 98, 309-312, (1928).

[15] P. Lancaster, K. Salkauskas, Surfaces generated by Moving Least Squares Methods, Mathematics of Computation, 155, 37, 141-158 (1981).